DOI: 10.13009/EUCASS2023-280
Aerospace Europe Conference 2023 – 10TH EUCASS – 9TH CEAS

Throttling hot-firing tests of methane engine thrust chamber with uni-element shear coaxial injector

Cheolwoong Kang, Shinwoo Lee*, Hadong Jung*, Sunwoo Han*, Kangyeong Lee*, Dongwoo Choi*, Changyoung Oh* and Kyubok Ahn*†*

** School of Mechanical Engineering, Chungbuk National University*

Chungdae-ro 1, Seowon-Gu, Cheongju, Chungbuk, 28644, Korea

kbahn@cbnu.ac.kr

† Corresponding Author

Abstract

In this study, the effect of recess length on the combustion characteristics of an injector used in a methane engine was investigated. Injectors without recess and with recess were manufactured, and these were mounted in a uni-element thrust chamber fueled by methane. Considering the operating conditions, tests were carried out under various mixture ratios and combustion chamber pressure ranges. The combustion efficiency and heat flux were higher as the recess length was longer. More stable combustion was achieved in injectors with recess regions. It was verified that the recess length had a positive effect on the combustion characteristics.

1. Introduction

In recent years, space development has become more competitive in terms of performance and cost rather than national competition. With the growth of the space industry, space agencies and companies are focusing their efforts on developing reusable launch vehicles to reduce costs, and are very interested in using methane as a fuel. Various companies in the United States are developing launch vehicles that use reusable methane as fuel. Research is also being conducted in Europe, Russia, China, and Japan to develop methane engines for competitive advantage. In an expander cycle methane engine using liquid oxygen and liquid methane as propellants, liquid methane passes through a regenerative cooling channel to cool the high-temperature combustion chamber, and is phase changed and supplied to the turbine and injector in a supercritical gas state. So, the propellant in the injector is liquid oxygen/gaseous methane, which is a liquid/gas combination. In liquid/gas propellant combinations, shear coaxial injectors are commonly used due to their simple structure and proven atomization and mixing performance.

The shear coaxial injector is divided into an inner injector part and an outer injector part, both of which have the same center axis. The atomization of liquid propellant in a shear coaxial injector is achieved by the difference in velocity and density of the propellant injected axially from the inner and outer injectors. Generally, a low-speed liquid oxidizer is injected from the inner injector and a high-speed gaseous fuel is injected annularly from the outer injector, which generates a shear force between the two propellants, which causes instability on the surface of the liquid jet and causes it to split into droplets. The better the atomization performance, the larger the surface area to mass ratio of the droplets, which improves evaporation, mixing, and combustion performance. The atomization and mixing performance of propellants is strongly influenced by the recess length, which is a geometric design parameter of the injector and has been studied extensively. The presence of recesses improves propellant atomization and mixing performance, increasing combustion efficiency and heat flux, and leading to more stable combustion [1-8]. However, previous studies have addressed the effects of recess length variation on combustion performance and combustion stability under specific operating conditions (narrow combustion chamber pressure and mixture ratio ranges).

The objective of this study is to determine the combustion characteristics of a shear coaxial injector with recess length under different operating conditions (wide range of combustion chamber pressures and mixture ratio conditions). For this purpose, a uni-element thrust chamber was designed and manufactured. In this paper, flow-controlled hot-firing tests were conducted and the results were analyzed to investigate the effect of recess length on the combustion characteristic velocity, characteristic velocity efficiency, heat flux, and combustion stability of a shear coaxial injector under various combustion chamber pressures and mixture ratios.

DOI: 10.13009/EUCASS2023-280

2. Uni-element thrust chamber and hot-firing test methods

2.1 Uni-element thrust chamber

The uni-element thrust chamber designed and manufactured to verify the combustion characteristics with the recess length of the injector was modeled on a 3-tonf methane engine with an expander closed cycle. The full-scale 3-tonf methane engine with a target specific impulse of 360 s was conceptually designed to have a combustion chamber pressure of 45 bar, a mixture ratio of 3.4, and 60 injectors. Figure 1 is a schematic of the designed uni-element thrust chamber. The thrust chamber consists of a head part containing the injectors, a combustion chamber part, and a nozzle part, each assembled with bolts, nuts, and copper gaskets.

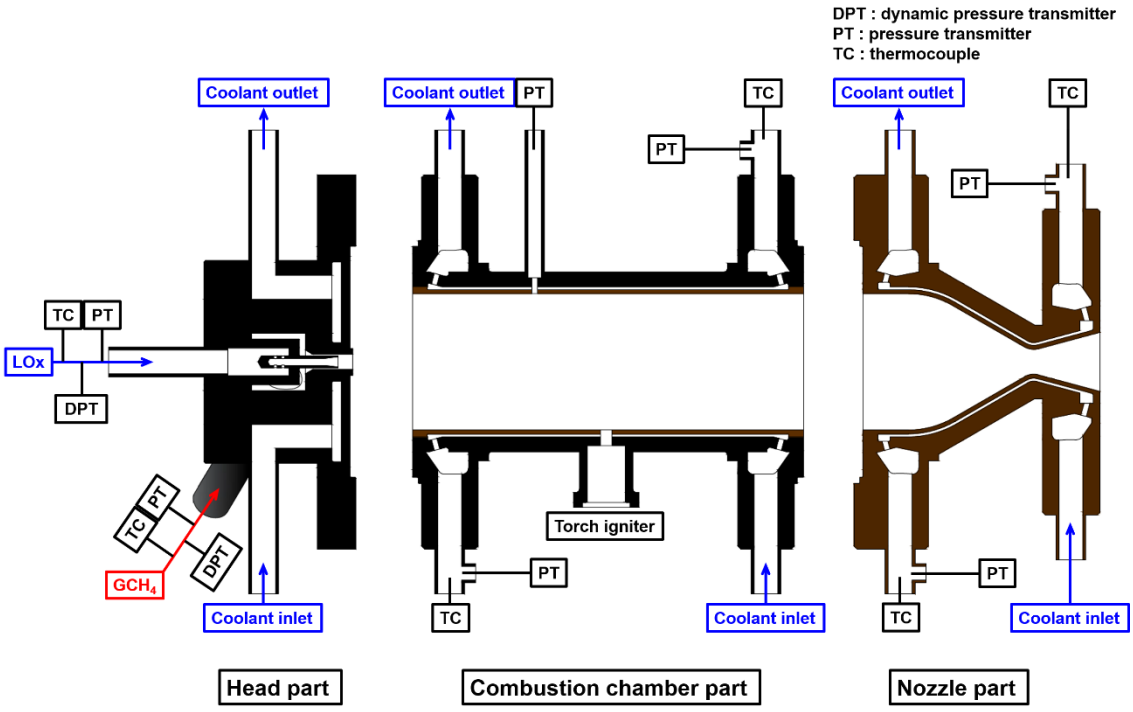

Figure 1: Schematic of the uni-element thrust chamber

Figure 2 shows a schematic of the shear coaxial injector used in this study, and Table 1 lists the injector design parameters and dimensions. A total of three shear coaxial injectors were manufactured, each with recess lengths of 0.0 mm, 2.5 mm, and 5.0 mm. The supplied liquid oxygen enters the inner injector in four holes through the oxidizer manifold and is discharged into the combustion chamber, while the gaseous methane is injected through the annular flow path of the outer injector. The faceplate of the thrust chamber head is cooled by cooling water through the cooling channels of the nozzle and combustion chamber parts as shown in Figure 1.

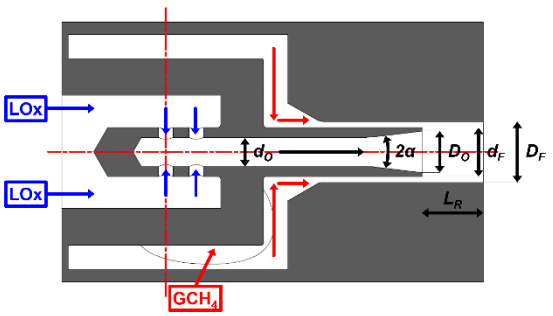

Figure 2: Schematic of the shear coaxial injector

DOI: 10.13009/EUCASS2023-280

Parameter	Unit	Injector No.		
		Inj#A	Inj#B	Inj#C
D_F	mm	5.0		
D_O		3.4		
d_F		4.0		
d_O		2.4		
L_R		0.0	2.5	5.0
2α	°	15		

Table 1: Design parameters and dimensions of injectors

The combustion chamber and nozzle parts of the combustion chamber of the uni-element thrust chamber are designed and manufactured to have cooling channels that simulate a regenerative cooling combustion chamber. The combustion chamber section has 60 straight cooling channels with a height of 1.00 mm and a width of 1.28 mm. The inner shell is made of copper alloy and the outer shell is made of UNS 31803, machined and brazed together. The combustion chamber is machined with ports for installing the torch igniter used for ignition of the main propellant, ports for cooling water inlet and outlet, and ports for measuring combustion chamber pressure and temperature/pressure at the cooling channel inlet and outlet. The nozzle is made by additive manufacturing using copper powder. The nozzle section is expanded and contracted along the axis to change the internal diameter, so the width of the cooling channel is also changed. To solve the problem of excessively small channel width at the nozzle throat, the height of the cooling channel was fixed at 1.50 mm and the thickness of the rib at 1.05 mm, and the number of cooling channels was smoothly reduced from 38 to 19 through additive manufacturing. Thus, 38 cooling channels start upstream of the nozzle and change to 19 cooling channels near the nozzle throat. The channel width varies accordingly: 3.10 mm → 1.10 mm → 3.15 mm → 1.00 mm (nozzle throat) → 3.10 mm. The nozzle is also machined with ports for cooling water inlet and outlet, and ports for measuring temperature/pressure at the cooling channel inlet and outlet.
The length of the thrust chamber head from the faceplate to the nozzle throat is 188.50 mm and the combustion chamber diameter is 45.75 mm. The design nozzle throat diameter is 8.36 mm, and the nozzle outlet diameter is 21.10. The cooling water supplied downstream of the nozzle was discharged upstream after passing through the nozzle cooling channel, and then supplied downstream of the combustion chamber to pass through the combustion chamber cooling channel and discharged upstream. Figure 3 is a photograph of the uni-element thrust chamber installed on a test stand.

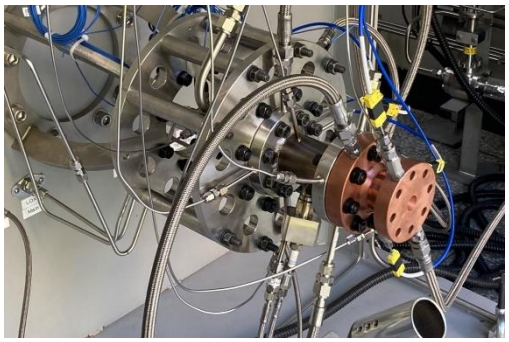

Figure 3: Schematic of the shear coaxial injector

2.2 Hot-firing test methods

The hot-firing test of the uni-element thrust chamber was conducted at the 1 kN class methane engine combustion test facility at Chungbuk National University. Liquid oxygen, the main propellant, is charged in the LOx run tank and pressurized with high-pressure gaseous nitrogen, and gaseous methane is stored in a high-pressure vessel and supplied under reduced pressure through a pressure regulator. The gaseous oxygen and gaseous methane for the torch igniter, which is used to ignite the main propellant, is also stored in a high-pressure vessel, supplied under reduced pressure through a pressure regulator, and ignited by a spark plug. In addition, manual valves, solenoid valves, and automatic pneumatic valves are operated to supply the main propellant and the propellant for the torch igniter. The automatic pneumatic valve is operated according to a pre-configured cyclogram in the LabVIEW program and a hot-firing test is performed.

DOI: 10.13009/EUCASS2023-280

Temperature, pressure, and flow data were obtained at a sampling rate of 100 Hz, while dynamic pressure data were recorded at a sampling rate of 10,000 Hz. The measured dynamic pressure data were band-pass filtered in the range of 30 to 4,999 Hz to remove unwanted noise. K-type thermocouples (Sentech SEN-320-S, uncertainty: ±1.5 K) and pressure transmitters (Sensys PSH series, uncertainty: ±0.15%) were installed at the manifold of the combustor head and at the inlet/outlet of the cooling channel to measure the temperature/pressure of the propellant and coolant. In addition, dynamic pressure sensors (PCB Piezotronics 102A14/102B, uncertainty: ±1.0%) were installed in the manifolds of each propellant to measure pressure perturbations. To measure the flow rate of the main propellant, a Coriolis mass flow meter (Micro Motion CMF025M, uncertainty: ±0.10%) and a venturi flow meter (Kometer GSAV-4000-S, uncertainty: ±1.0%) were installed in series in the oxidizer line and a Bronkhorst mass flow meter (Bronkhorst M55, uncertainty: ±0.5%) and a venturi flow meter (Kometer GSAV-4000-S, uncertainty: ±1.0%) in the main fuel line. A turbine flow meter (Kometer NK-250, uncertainty: ±0.5%) was used to measure the coolant flow. A detailed description of the hot-firing test rig can be found in the references [9,10].
The hot-firing tests with varying mixture ratios and combustion chamber pressures were conducted independently, and the hot-firing test conditions are shown in Figure 4. The first hot-firing test for each injector was performed at a fixed combustion chamber pressure with successive 0.34 mixture ratio increments, from a 20% reduction in mixture ratio to a 20% increase in mixture ratio relative to the design point. The other hot-firing test was performed at a fixed mixture ratio with successive decreases of 9 bar in combustion chamber pressure, from 100% combustion chamber pressure to 20% combustion chamber pressure at DP.

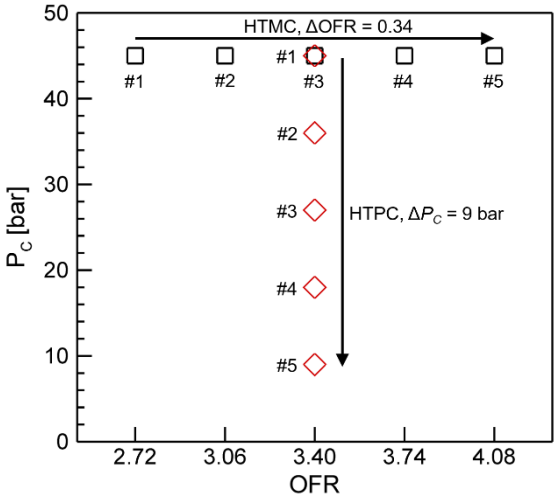

Figure 4: Condition of the hot-firing test

3. Hot-firing test results

3.1 Hot-firing tests

The hot-firing test with the mixture ratio changed is named HTMC (hot-firing test of mixture ratio-controlled), and the hot-firing test with the combustion chamber pressure changed is named HTPC (hot-firing test of pressure-controlled). Figure 5is a video of the Inj#A_HTPC hot-firing test. As the combustion chamber pressure is lowered, the length of the exhaust plume at the nozzle exit is shortened.

DOI: 10.13009/EUCASS2023-280

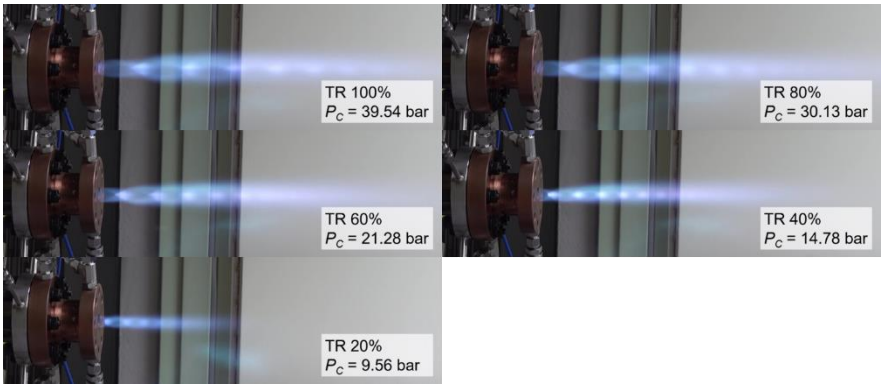

Figure 5: Snapshot of Inj#A_HTPC hot-firing test

The combustion chamber pressure, propellant mass flow rate, and flow control valve stroke values for the Inj#A injector hot-firing test are shown in Figure 6. Figure 6(a) is the result of the Inj#A_HTMC hot-firing test. From 0 to 4 seconds, a nitrogen purge is performed to remove dust and residual propellant that may be present in the piping and thrust chamber head. From 4 to 9 seconds, the torch igniter is activated, and at approximately 7 seconds, the main ignition is achieved with the supply of liquid oxygen and gaseous methane, and the combustion chamber pressure is raised. The black vertical dotted line is the point at which the stroke of the flow control valve is changed. The stroke of the oxidizer flow control valve was gradually increased and the stroke of the fuel flow control valve was gradually decreased to change the propellant flow rate in order to change the mixing ratio, and it can be seen that the propellant flow rate changes. Figure 6(b) shows the results of the Inj#A_HTPC hot-firing test, where both the oxidizer and fuel flow control valve strokes were decreased to reduce the total propellant mass flow rate, resulting in a decrease in propellant mass flow rate and a decrease in combustion chamber pressure.

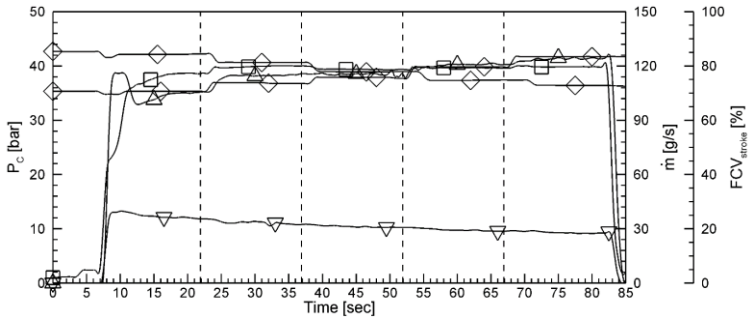

(a)

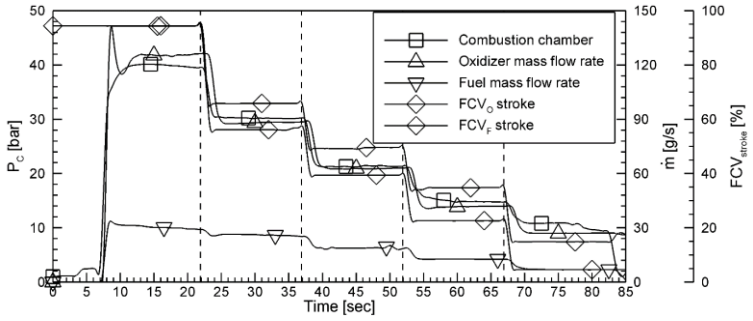

(b)

Figure 6: Combustion chamber pressure, propellant mass flow rate, and FCV stroke: (a) inj#A_HTMC and (b) inj#A_HTPC

All data for each hot-firing test was averaged over the 0.2-second section before and after the 1-second period when the flow control valve's set stroke changed to minimize noise. Figure 7 shows the combustion chamber pressure and mixture ratio results for all hot-firing tests. It can be seen that for the HTMC test, the mixture ratio changes while the combustion chamber pressure remains almost constant, and for the HTPC test, the combustion chamber pressure

DOI: 10.13009/EUCASS2023-280

gradually decreases while the mixture ratio remains almost constant. The injection pressure drop with oxidizer mass flow rate for each hot-firing test is summarized in Figure 8. Looking at the injection pressure drop, HTMC shows an overall increase in injection pressure drop with increasing propellant mass flow rate. However, for HTPC, the injection pressure drop increases in the low-combustion chamber pressure range. This is due to the decreased mass flow rate of the oxidizer, lower combustion chamber pressure, and reduced pressure in the oxidizer manifold, resulting in the supply of gaseous oxygen instead of liquid oxygen.

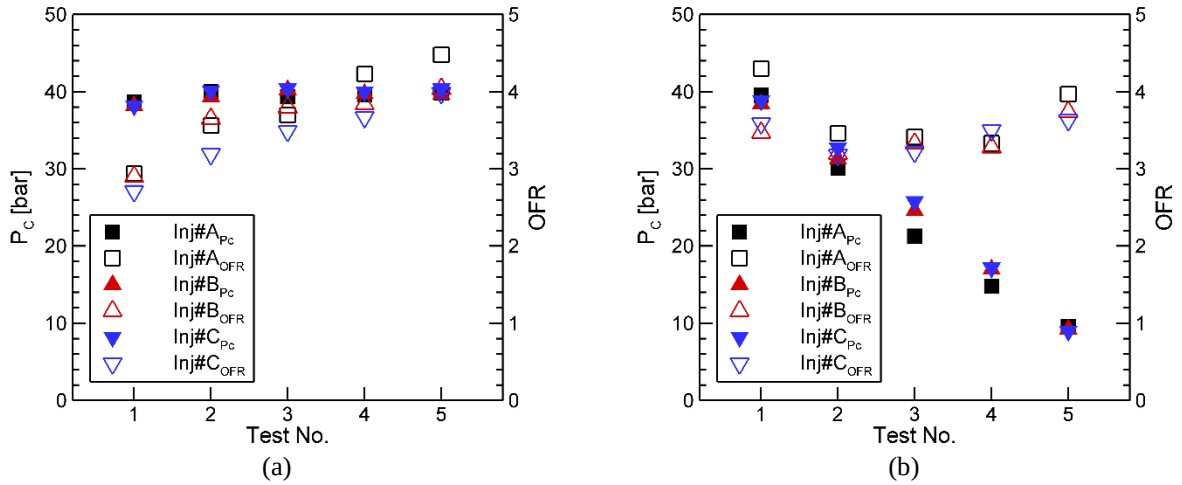

Figure 7: Combustion chamber pressure and mixture ratio: (a) HTMC and (b) HTPC

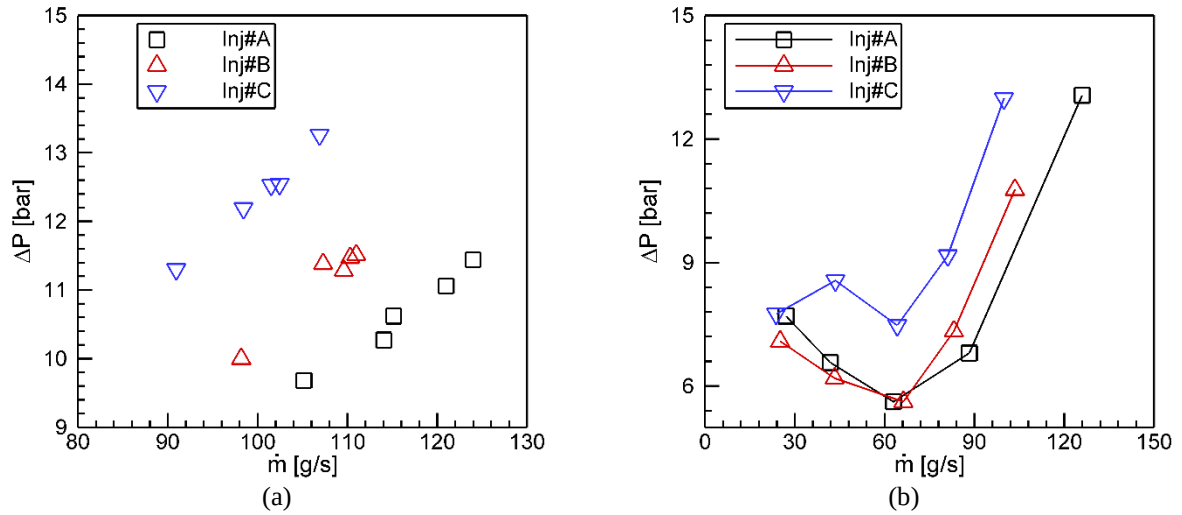

Figure 8: Injector pressure drop of all hot-firing tests: (a) HTMC and (b) HTPC

3.2 Combustion characteristics

The performance of the engine is mainly judged by the specific impulse, and thrust measurement is required to obtain the specific impulse. In this study, a nozzle with a small nozzle expansion ratio was used because we are focused on combustion performance, so the combustion characteristic velocity efficiency is used as a criterion for combustion performance. The experimental characteristic velocity ($C^*_{exp.}$) is calculated from the combustion chamber pressure (P_C) and total propellant mass flow rate ($\dot{m}_t$) measured during the hot-firing test, and the nozzle throat area (A_t) measured after the hot-firing test, as shown in Eq. 1. The characteristic velocity efficiency (η_{C^*}) is the ratio of the theoretical characteristic velocity (C^*_{ideal})to the actual characteristic velocity, calculated as Eq. 2. The theoretical characteristic velocity can be obtained by entering the combustion chamber pressure, total propellant mass flow rate, mixture ratio, nozzle contraction ratio, and nozzle expansion ratio into a RPA (rocket propulsion analysis) program [11], [12].

DOI: 10.13009/EUCASS2023-280

$$C^*_{exp.} = \frac{P_C \times A_t}{\dot{m}_t} \tag{1}$$

$$\eta_{C^*} = \frac{C^*_{exp.}}{C^*_{ideal}} \tag{2}$$

Figure 9 shows the characteristic velocity and characteristic velocity efficiency. The dotted line is the average characteristic velocity efficiency. From Figure 9(a) and (b), it can be seen that there is no difference between the actual characteristic velocity and characteristic velocity efficiency as the mixture ratio changes as a result of HTMC, and the combustion performance is higher in the injector with a longer recess length. The characteristic velocity efficiency for Inj#A, Inj#B, and Inj#C were 84.48%, 90.37%, and 95.47%, respectively. Compared to the Inj#A injector, the combustion efficiency of the Inj#B injector is improved by 5.89%, and the Inj#C injector is improved by 5.1% compared to the Inj#B injector. This is believed to be the result of rapid atomization and mixing due to the propellant collision in the recess area, resulting in improved combustion performance. Figures 9(c) and (d) show that the combustion performance is maintained regardless of thrust as a result of HTPC, and similarly, the combustion efficiency is improved by about 5% as the recess length increases. However, for combustion chamber pressure ratios of 20% and 40%, it can be seen that the actual characteristic velocity and efficiency are similar regardless of the injector. It is believed that the combustion efficiency is increased by supplying gaseous oxygen instead of liquid oxygen as the flow rate of the oxidizer is reduced, and it is expected that the efficiency is higher in the thrust condition below 20%.

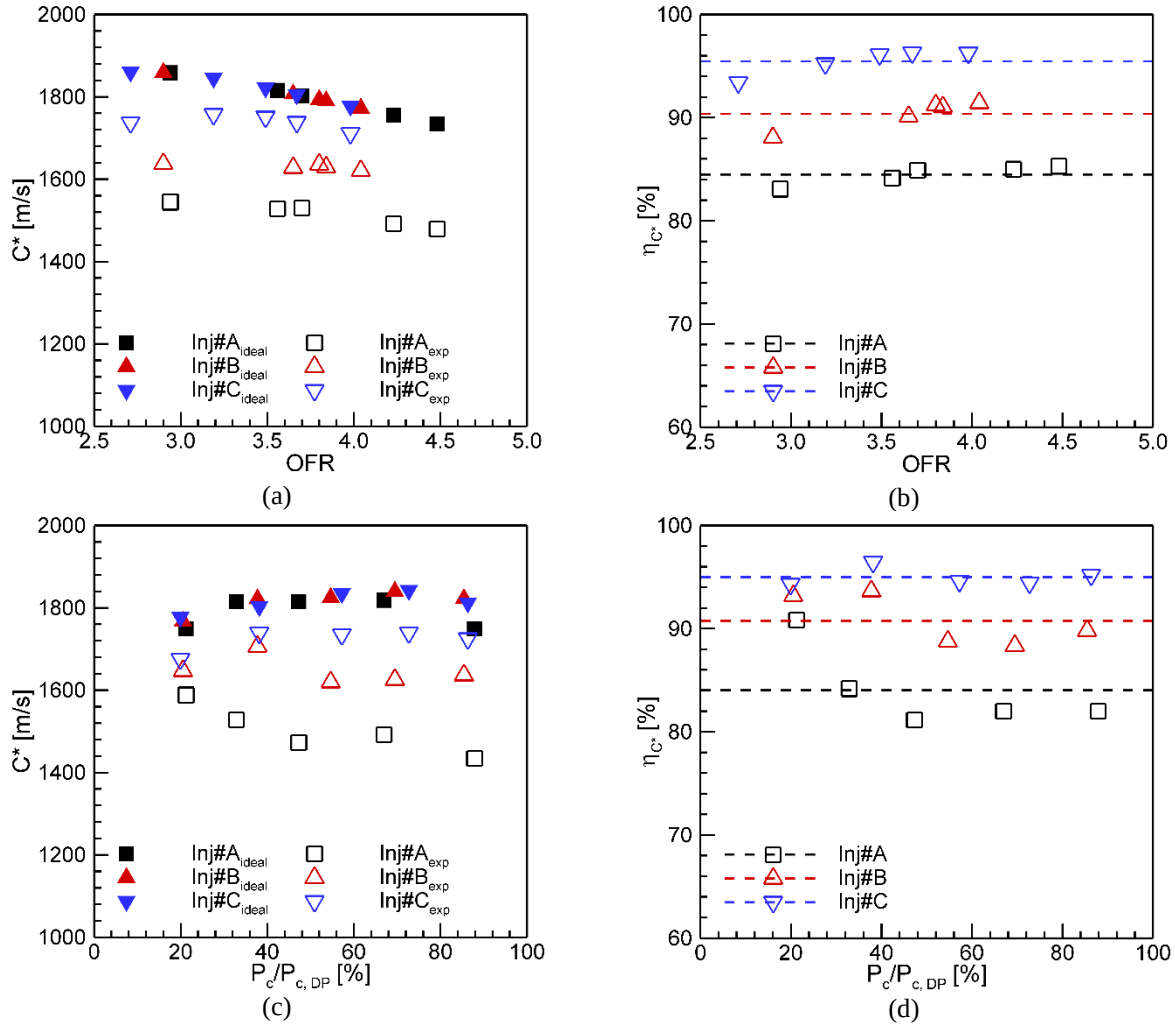

Figure 9: Combustion performance: (a), (b) HTMC and (c), (d) HTPC

Figure 10 shows the temperature variation of the coolant during the hot-firing test. As mentioned in Section 2, the coolant supplied from the downstream of the nozzle passes through the cooling channel of the nozzle and is discharged

DOI: 10.13009/EUCASS2023-280

from the upstream of the nozzle, and then enters the downstream of the combustion chamber and is discharged from the upstream. Therefore, the temperature increases in the following order: downstream of the nozzle, upstream of the nozzle, downstream of the combustion chamber, and upstream of the combustion chamber. Looking at the results of the HTMC hot-firing test, it can be seen that the temperature of the coolant does not change much as the mixture ratio changes. However, in the case of the HTPC hot-firing test, the temperature variation of the coolant gradually becomes smaller as the combustion chamber pressure decreases. The heat flux ($\ddot{q}$) is calculated from the mass flow rate of the coolant ($\dot{m}_{coolant}$), the specific heat of constant pressure (c_p), the temperature variation (ΔT), and the internal area of the combustion chamber (A_{inner}) as shown in Eq. 3, and the results are shown in Figure 11 and Figure 12.

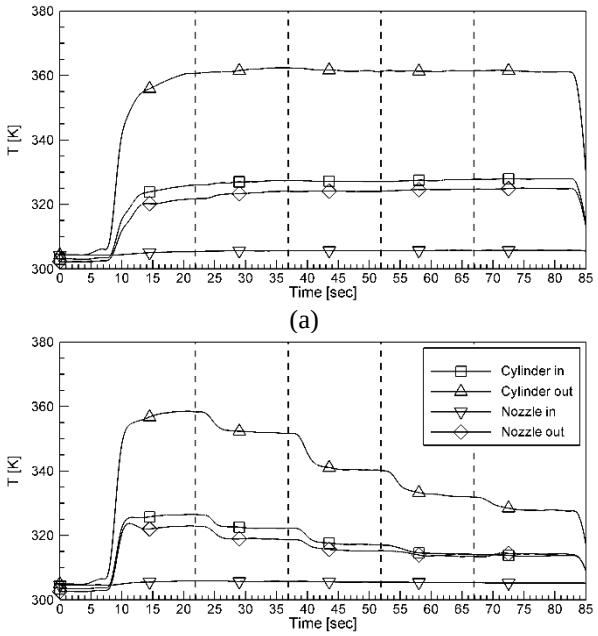

Figure 10: Coolant temperature variation: (a) inj#A_HTMC and (b) inj#A_HTPC

$$\ddot{q} = \frac{\dot{m}_{coolant} \times c_p \times \Delta T}{A_{inner}} \tag{3}$$

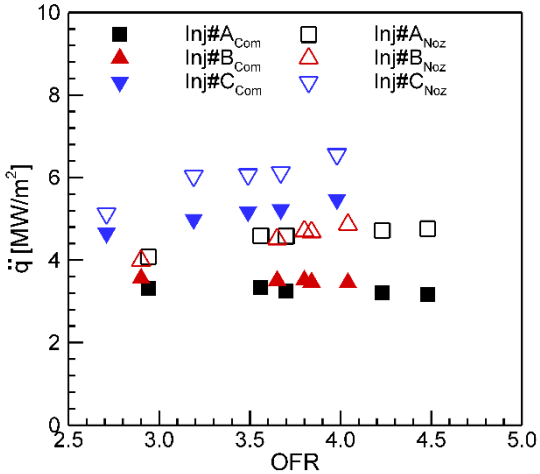

Figure 11: Heat flux of HTMC hot-firing test:

Since the temperature and pressure were measured only at the inlet and outlet of the cooling channel of the combustion chamber and the nozzle respectively in this study, the heat flux means the average heat flux of the combustion chamber and the nozzle. Therefore, the heat flux in the nozzle section is higher than the heat flux in the combustion chamber section because there are nozzle throat in the nozzle section where the heat load is most concentrated [13], [14]. In Figure 11, there is no significant change in heat flux with the mixture ratio, and the combustion chamber pressure is

DOI: 10.13009/EUCASS2023-280

almost constant, so the heat flux does not change. However, the Inj#C injector with the longest recess length recorded the highest heat flux. Figures 12(a) and (b) show the heat flux at the combustion chamber and nozzle, respectively, as a result of HTPC. It has been shown that the heat flux changes proportionally to the combustion chamber pressure, as shown in the bartz equation. It can be seen that the heat flux in the combustion chamber increases as the recess length increases. This is thought to be due to the fact that as the recess length increases, the length of the flame becomes shorter and wider, allowing it to directly contact the inner wall of the combustion chamber, increasing the heat flux. On the other hand, if we look at the heat flux at the nozzle, we can see that the difference between Inj#A and Inj#B is not significant, and Inj#C has a significant increase. According to reference [6], as the recess length increases, the heat flux increases in the entire area, and the localized heat flux region moves downstream of the combustion chamber. Therefore, it is judged that the heat flux increased with the recess length in the combustion chamber part, and the heat flux increased sharply only in Inj#C in the nozzle part.

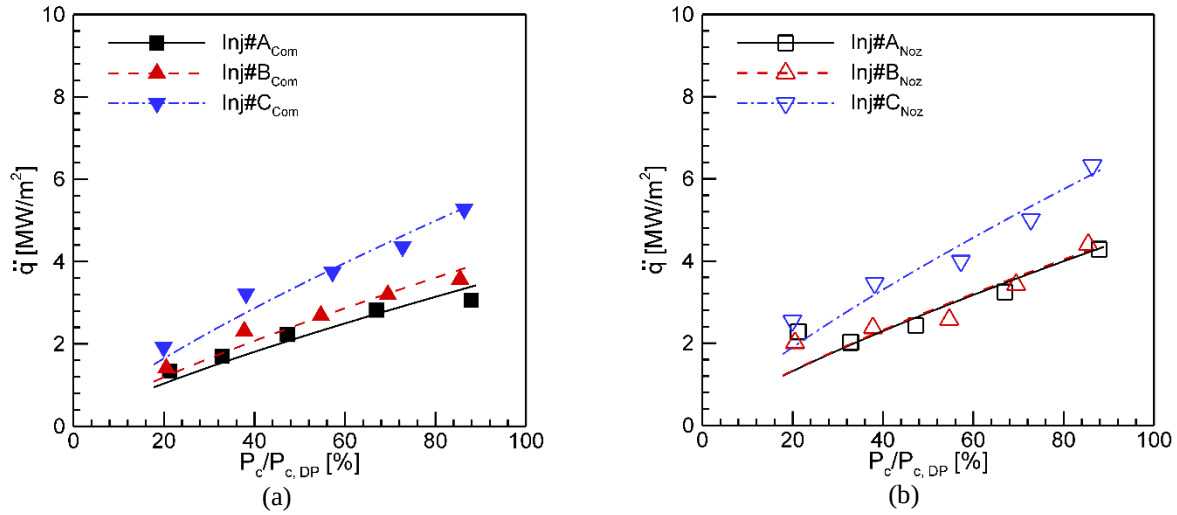

Figure 12: Heat flux of HTPC hot-firing test: (a) combustion chamber and (b) nozzle

A small pressure drop across the injector minimizes the weight of the injector and the requirements on the supply system, but as a rule of thumb, the pressure drop across the LOx injector should be kept between 15% and 20% to prevent interaction between the combustion gases and the supply system. However, it is known that combustion instability can occur in the low thrust range, i.e., at low combustion chamber pressures, when the pressure in the LOx manifold becomes lower than at full thrust and falls below a critical pressure, depending on the propellant mixture ratio. Liquid rocket engines with adjustable thrust are particularly susceptible to low-frequency combustion instability, known as chug, in the low-thrust range. Figure 13 shows the RMS value of pressure fluctuation (p'_{rms}) versus average combustion chamber pressure($\bar{P}_C$) for all hot-firing tests. In conclusion, in this study, the RMS value of pressure fluctuation versus mean combustion chamber pressure was up to 0.45%, which is below the criterion for combustion instability (p'_{rms}/P_C < 3%) [15]. It is believed that the oxidizer vaporizes in the low combustion chamber pressure region and the pressure in the oxidizer manifold rises, increasing the differential pressure, so that low-frequency combustion instability did not occur. The difference in the RMS value of the pressure fluctuation versus the average combustion chamber pressure for the three injectors is very small, but the value for the Inj#A injector without recess appears to be large. It can be concluded that the presence of the recess improves combustion stability.

DOI: 10.13009/EUCASS2023-280

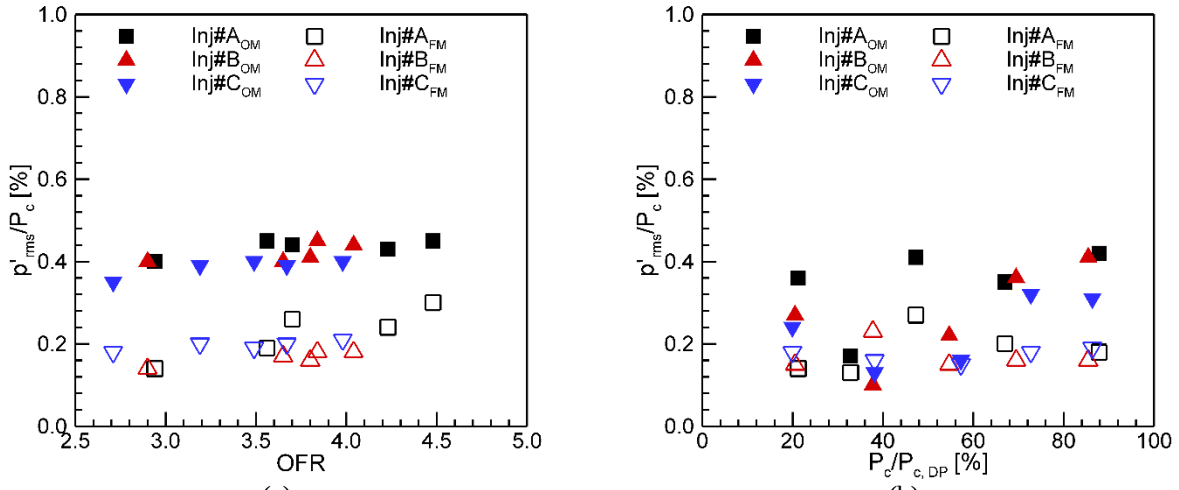

Figure 13: $p'_{rms}/\bar{P}_C$: (a) HTMC and (b) HTPC

4. Conclusion

Hot-firing tests were conducted to examine the effect of recess length for shear coaxial injectors at various mixture ratios and combustion chamber pressure conditions. First, the performance was found to be consistent at various mixture ratios and combustion chamber pressure conditions, except for the 20% and 40% combustion chamber pressure conditions. At the combustion chamber pressure of 20% and 40%, the oxidizer feed flow was lower, resulting in improved performance due to the oxidizer being supplied as gaseous oxygen rather than liquid oxygen. The presence of the recess area had three consequences. First, it improved propellant atomization and mixing performance, which in turn improved combustion efficiency. Second, the presence of the recess enlarged the flame structure and shifted the localized heat flux region downstream of the thrust chamber, resulting in very high heat fluxes at the longest recess lengths. These results, as noted in other papers, should be considered in the design of cooling systems. Third, the injectors with recesses showed slightly better combustion stability than those without recesses.

References

[1] Tani, H., S. Teramoto, and K. Okamoto. 2015. Effects of injector geometry on cryogenic shear coaxial jets at supercritical pressures. J. Propuls. Power. 31(3):883–888.
[2] Gill, G. S., and W. H. Nurick. 1976. Liquid Rocket Engine Injectors. NASA-SP-8089.
[3] Lux, J., and O. Haidn. 2009. Effect of recess in high-pressure liquid oxygen/methane coaxial injection and combustion. J. Propuls. Power. 25(1):24–32.
[4] Silvestri, S., M. P. Celano, C. Kirchberger, G. Schlieben, O. Haidn, and O. Knab. 2016. Investigation on Recess Variation of a Shear Coax Injector for a Single Element GOX-GCH4 Combustion Chamber. Trans. Japan Soc. Aeronaut. Sp. Sci. Aerosp. Technol. Japan. 14(ists30):Pa_13-Pa_20.
[5] Silvestri, S., F. Winter, M. Garulli, M. P. Celano, G. Schlieben, O. Haidn, and O. Knab. 2017. Investigation on Recess Variation of a Shear Coaxial Injector in a GOX-GCH4 Rectangular Combustion Chamber with Optical Access. In: 7th European Conference for Aeronautics and Aerospace Sciences. EUCASS 2017-242.
[6] Song, J., and B. Sun. 2016. Coupled heat transfer analysis of thrust chambers with recessed shear coaxial injectors. Acta Astronaut. 132:150–160.
[7] Woodward, R. D., S. Pal, S. Farhangi, G. E. Jensen, and R. J. Santoro. 2007 LOX/GH2 shear coaxial injector atomization studies: Effect of recess and non-concentricity. In: 45th AIAA Aerospace Sciences Meeting and Exhibit. AIAA 2007-571.
[8] Muto, D., H. Terashima, and N. Tsuboi. 2016. Characteristics of Jet-Mixing at Supercritical Pressure: Effects of Recess Length and Post Height. Trans. Japan Soc. Aeronaut. Sp. Sci. Aerosp. Technol. Japan. 14(ists30):Pa_45-Pa_52.
[9] Kang, C., D. Hwang, J. Ahn, J. Lee, D. Lee, and K. Ahn. 2021. Methane Engine Combustion Test Facility Construction and Preliminary Tests. J. Korean Soc. Propuls. Eng. 25(3):89–100.
[10] Kang, C., S. Lee, S. Han, K. Lee, H. Jung, D. Choi, and K. Ahn. 2023. Step-by-step Tests for Continuous Thrust Control Hot-firing Test. J. Korean Soc. Propuls. Eng. 26(1):58-67.

DOI: 10.13009/EUCASS2023-280

[11] Ponomarenko, A. 2010. RPA: Tool for Liquid Propellant Rocket Engine Analysis C++ Implementation.
[12] Ponomarenko, A. 2014. RPA-Tool for Rocket Propulsion Analysis. In: Space Propulsion Conference.
[13] Sutton, G. P., and O. Binlarz. 2020. Rocket Propulsion Elements. 9th ed. John Wiley & Sons.
[14] Leccese, G., D. Bianchi, B. Betti, D. Lentini, and F. Nasuti. 2018. Convective and radiative wall heat transfer in liquid rocket thrust chambers. J. Propuls. Power. 34(2):318–326.
[15] Klem, M. D., and R. S. Fry. 1997. Guidelines for Combustion Stability Specification and Verification Procedures for Liquid Propellant Rocket Engines. CPIA publication 665.